J Solid State Electrochem (2011) 15:1109–1113
DOI 10.1007/s10008-010-1167-9

ORIGINAL PAPER

Dependence of RuO_2-capacitive properties on preparation conditions

Leonardo A. Pocrifka · Renato G. Freitas · Adriane V. Rosario · Ernesto C. Pereira

Received: 8 March 2010 / Revised: 4 August 2010 / Accepted: 4 August 2010 / Published online: 24 August 2010

Abstract The effect of a small change in the preparation conditions and the consequences thereof on the capacitive properties of RuO_2 thin films are described. The oxide films are prepared using the Pechini method and the only alteration made in the procedure is to change the order of addition of reagents. The solution color changes as a consequence and also the capacitance values, from 54.8 to 33.6 F g^{-1}, for the oxides obtained after calcination. These results could be related to the calcination kinetics, which affects the lattice stress in the oxide as calculated using X-ray diffraction patterns and Rietveld analysis.

Keywords Electrochemical capacitors · Ruthenium oxide · Sol-gel route · Pechini method · Electrochemical properties · Rietveld analysis

Introduction

The search for alternative sources of energy with low environmental impact is a global concern. In recent years, research into electrochemical capacitors has increased significantly due to their potential use as auxiliary power sources in hybrid systems that require pulses of energy [1]. Electrochemical capacitors are also attractive power sources for such varying applications as camera flashes, lasers, and electronic equipment [2, 3]. These devices are separated into two different categories: (1) double-layer capacitors, which are generally based on carbon with high specific area and involve charge storage in the double layer at the electrode/electrolyte interface [4, 5]; and (2) redox capacitors, which are based on the pseudocapacitance of materials in which redox reactions occur at the electrode surface. According to the literature, different materials, such as hydrogen–metal systems [6], conducting polymers [7–9], and transition metal oxides (IrO_2 [10], MnO_2 [11], SnO_2 [12], NiO_x [13], and RuO_2 [14–16]), can be used to build these devices.

Ruthenium oxide is recognized as the most promising material for high energy and power density devices due to its capacitive behavior and its stability through a wide potential range with high reversibility, in addition to long cycle life and high conductivity [17]. Although ruthenium compounds are expensive, the improved performance of RuO_2 capacitors justifies their use. This oxide has been prepared using various methods and it has been demonstrated that capacitance is highly dependent on the preparation method. Specific capacitances around of 720 F g^{-1} have been obtained using electrodes of hydrous ruthenium oxide (RuO_2nH_2O) [18, 19]. Using a different preparation method, cathodic electrodeposition of the oxide on titanium substrate [20], a specific capacitance of 788 F g^{-1} was observed. Finally, materials synthesized under hydrothermal conditions have also been suggested to prepare these devices [21, 22]. In order to decrease the device cost, binary materials, such as RuO_2–SnO_2 [23], have also been proposed. This binary oxide presented reversible behavior and high energy with specific capacitance of 830 F g^{-1} for a $RuO_{0.6}Sn_{0.4}O_2nH_2O$ film. A preparation route using a solid-state procedure led to the synthesis of nanoscale RuO_2nH_2O [24]. This procedure involves a simple mixture of the $RuCl_3{\cdot}xH_2O$ with ethanol at room temperature. In this case, a study of the thermal treatment temperature effect was also carried out, and the

L. A. Pocrifka · R. G. Freitas · A. V. Rosario · E. C. Pereira (✉)
NANOFAEL-LIEC, Departamento de Química,
Universidade Federal de São Carlos,
C.P.: 676—CEP 13565-905,
São Carlos, São Paulo, Brazil
e-mail: decp@ufscar.br

results showed that the RuO_2nH_2O powder synthesized at 150 °C was amorphous with a maximum capacitance of 655 F g^{-1}. At higher temperatures, the capacitance values decreased drastically due to the increase of the crystalline portion of the material. Using a single-step chemical method, amorphous RuO_2 thin films were obtained on different substrates [25] and a specific capacitance of 50 F g^{-1} was observed.

Another preparation route is the polymeric precursor method (PPM), which involves the polymerization of organic monomers in the presence of metal ions, which are homogeneously distributed between the polymeric chains that are then thermal-treated to obtain an oxide film or powder. In this method, citric acid (CA) and ethylene glycol (EG) are used to prepare a polymeric precursor, and the metal is complexed with the solution components leading to a random distribution of the metal ions in the polymeric network [26]. Different materials for electrochemical applications, such as dimensionally stable anodes [27, 28], electrochromic materials [29], pH electrodes[30, 31], and electrochemical capacitors[32], have been prepared using this procedure. The effect of the calcination temperature on the capacitive properties of prepared RuO_2 thin films [5] showed that the best material results, 70 F g^{-1}, were obtained using a calcination temperature of 250 °C. The main advantages of PPM are its low price, ease of preparation, and the possibility to prepare low-level doped materials. Moreover, as we will present in this study, many experimental variables can be controlled, leading to important modifications in the material properties.

Considering what has been mentioned above, in this study, the polymeric precursor method was used to prepare ruthenium oxide thin films with identical composition while only the order of addition of reagents was altered. As will be shown, the prepared oxides have completely different electrochemical properties.

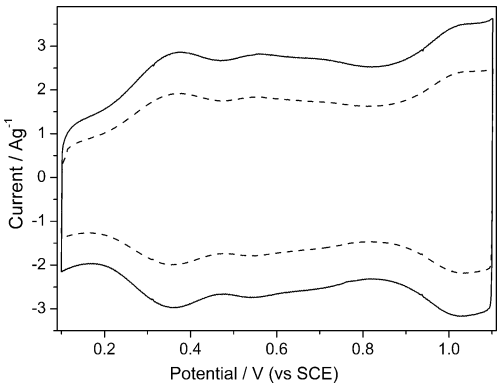

Fig. 1 Cyclic voltammograms of the RuO_2 electrodes in 1.0 mol L^{-1} H_2SO_4: (*broken line*) Ti/$RuO_{2(G)}$ and (*solid line*) Ti/$RuO_{2(B)}$, v= 50 mV s^{-1} at 25 °C

Table 1 Mass and capacitance values of the electrodes

Parameters	Brown electrode	Green electrode
Procedure	A	B
Mass/mg	0.7	1.0
Capacitance/F g^{-1}	54.8	33.6

Experimental

Two precursor solutions were prepared, each with a composition equal to 1:3:12 (Ru/CA/EG) molar ratio. The only difference between the procedures was the order of addition of reagents. In procedure A, the precursor solution was prepared by the addition of citric acid (Synth) to ethylene glycol (Mallinckrodt), stirring at 60 °C. Following this, the metal precursor, $RuCl_3nH_2O$ (Aldrich), was added to the solution. Both stirring and temperature were maintained at constant levels until the complete dissolution of the metal ions. In procedure B, the solution was prepared by the addition of $RuCl_3nH_2O$ to ethylene glycol, stirring at 60 °C. After this, citric acid was added. The two procedures led to solutions with different colors. The first procedure resulted in a brown solution, while the second procedure led to a green solution. The films obtained with these solutions were called $RuO_{2(B)}$ and $RuO_{2(G)}$, respectively. It is important to emphasize that, after thermal treatment, both materials had a dark brown color. Titanium plates with exposed areas of 1.0 cm^2 (99.7%, Ti-Brazil) were used as substrates to prepare the electrodes. The substrates were treated by sandblasting, followed by a chemical treatment in hot 5% (*w*/*v*) oxalic acid solution for 10 min, washed with Milli-Q water, and dried at 150 °C. The precursor solutions were painted over the substrate and then thermally treated at 110 °C for 30 min to promote polymerization, at 250 °C for 20 min to improve oxide adhesion to the substrate, and finally at 400 °C for 10 min. This deposition/calcination procedure was repeated five

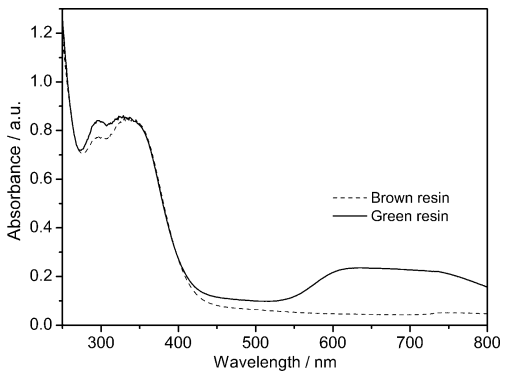

Fig. 2 Visible absorption spectra of the brown and the green precursor solutions

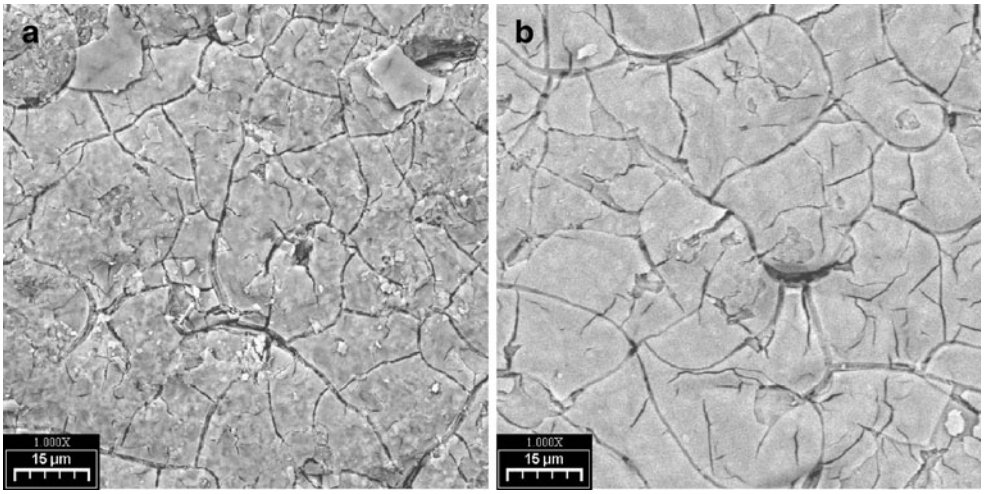

Fig. 3 SEM micrographs for **a** Ti/$RuO_{2(G)}$ and **b** Ti/$RuO_{2(B)}$ films

times in order to increase the oxide layer mass which was measured as 1.0 and 0.7 mg for $RuO_{2(G)}$ and $RuO_{2(B)}$, respectively. All samples were prepared in triplicate.

Electrochemical measurements were carried out using an Autolab potentiostat/galvanostat model PGSTAT20 in a single compartment cell using two platinum sheets as counter electrodes and a saturated calomel electrode as reference. The experiments were conducted in a 1.0-mol-L^{-1} H_2SO_4 solution. Prior to electrochemical measurements, the solution was bubbled with N_2 for 20 min.

Transmittance spectra of the solutions prepared using procedures A and B were measured using a UV–Vis–NIR spectrophotometer Cary model 5G. Sample morphologies were measured using a scanning electron microscope (SEM) Zeiss model 940A. The X-ray diffraction (XRD) patterns of the electrodes were obtained using a SIEMENS diffractometer model D-5000 with CuKα radiation and λ= 1.5406 Å. The range used was 2θ=20–130° with 0.02 increment steps. To analyze the XRD data, we used Rietveld refinement with the General Structure Analysis System program [33, 34].

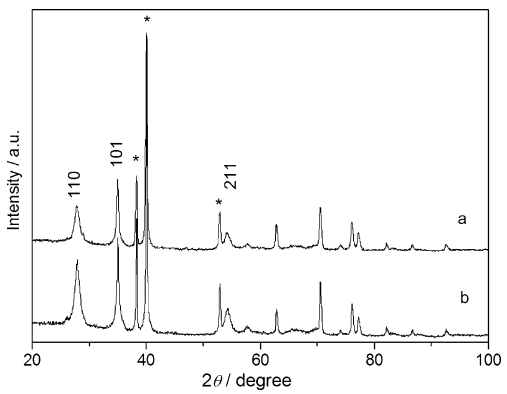

Fig. 4 XRD patterns of the RuO_2: *a* Ti/$RuO_{2(G)}$ electrode and *b* Ti/$RuO_{2(B)}$ electrode

Results and discussion

The electrodes were characterized by cyclic voltammetry measurements in an acid medium as shown in Fig. 1. The voltammetric profile observed for both electrodes indicated typical capacitive behavior of ruthenium oxide electrodes [35, 36]. Broad peaks appeared in the anodic and cathodic scans. RuO_2 pseudocapacitance was attributed to redox transitions, including Ru(II)/Ru(III), Ru(III)/Ru(IV), and Ru(IV)/Ru(VI) [37–40]. In this figure, it is shown that the oxide prepared with the brown solution led to a higher current density normalized by the deposited mass. Table 1 presents the specific capacitance, C_s, calculated by:

$$C_s = \frac{Q}{\Delta E \times m} \quad (1)$$

where Q in the voltammetric charge, ΔE is the potential window, and m is the RuO_2 mass. It was observed that the electrode prepared with the brown solution led to a capacitance 1.5 times higher than the electrode prepared with the green solution. It is important to point out that the electrodes were prepared from solutions with the same composition and using the same calcination process. The only difference between procedures A and B, as has been described in the "Experimental" section above, was the order of addition of reagents.

Neither the precursor solution composition nor the thermal treatment was modified. It is clear, therefore, that

Table 2 Diffraction parameters calculated using Rietveld method

Parameters	$RuO_{2(G)}$	$RuO_{2(B)}$
Phase	Rutile	Rutile
Grain size/nm	8.7	9.3
Stress/%	4.6	2.9

a different factor led to the changes observed in the final material. The different order of addition of reagents must, therefore, have produced an alteration in the structural and/or morphological characteristics of the oxide. In principle, the CA/EG ratio governs the polymerization and cross-linking degree of the precursor polyester chains, whereas the metal precursor concentration is responsible for the oxide nuclei density and oxide particle growth [41]. However, it was observed for different oxide systems that the CA/metal precursor ratio also plays a role during polymeric network formation [42]. It is possible, therefore, that the final oxide has its characteristics determined by the kind and degree of metal complexation with the chelant: in this case, citric acid. To investigate the effects producing differences in the electrode capacitance values, we used various techniques. UV–Vis absorption spectra are presented in Fig. 2 and two absorption band peaks at 320 and 350 nm can be observed. These bands are attributed to the (p) $\pi\rightarrow$(p) π^* internal transition (IL) of the ligand that is coordinated with ruthenium [43]. In addition to these absorption peaks, there is a broad band between 550 and 800 nm in the spectrum of the green solution (procedure B). The results indicate that during the preparation of the brown solution (procedure A), in which citric acid was added first to ethylene glycol and the esterification reaction occurred, the metal ions were mixed with this precursor solution and remained in the Ru^{3+} state. The metal in this oxidation state has an external shell structure d^5 and does not present any electronic metal–ligand charge transfer, MLCT, in the visible region [44]. However, in procedure B, in which the citric acid was added last, Ru^{3+} was reduced to Ru^{2+} due to the strong reducing power of citric acid. This hypothesis results from the appearance of the band in the 550–800-nm region. According to the literature, this band is attributed to the *Ru* (d) $\pi\rightarrow$(p) π^* MLCT transition. This is, therefore, a likely explanation for the solution color change. Moreover, although the solution compositions are the same, the initial state of metal ions and subsequently the metal complex are different for procedures A and B as a consequence. This change in the initial state of the preparation process could, therefore, lead to differences in the calcination process kinetics or mechanism, which could explain the changes in the oxide capacitance values.

Figure 3 presents the micrographs of $RuO_{2(G)}$ and $RuO_{2(B)}$. Both samples present a so-called mud crack morphology, which is common in dimensionally stable anodes. Comparing both figures, there are no significant differences that could explain the electrochemical behavior. In order to investigate the sample microstructures, X-ray diffraction measurements were performed (Fig. 4). In this figure, the most intense diffraction peaks are those related to metallic Ti (JCPDS file # 44-1294), indicating that the RuO_2 films are thin. Moreover, RuO_2 patterns are also observed at 2θ=28.009° (110), 2θ=35.050° (101), and 2θ=54.245° (211) in agreement with JCPDS file (PDF file # 40-1290). The diffraction data were analyzed using the Rietveld method and the data are presented in Table 2. As can be observed in Table 2, crystallite sizes (CS) for $RuO_{2(G)}$ and $RuO_{2(B)}$ (110) were 8.7 and 9.3 nm, respectively. This difference is within the experimental error of the Rietveld method and we can conclude, therefore, that the CS for both samples are the same and that the difference observed in the capacitance cannot be attributed to this microstructural characteristic. Furthermore, it is well known that changes such as crystal imperfections lead to strain in the crystal lattice, S. Analyzing the plane (110), the d-spacing changes from 3.207 to 3.178 Å for $RuO_{2(G)}$ and $RuO_{2(B)}$, respectively, compared to 3.183 Å JCPDS (PDF file # 40-1290), indicating that the lattices are stressed. The S values were then calculated using the Rietveld refinement and changes from 4.6% to 2.8% to $RuO_{2(G)}$ and $RuO_{2(B)}$, respectively, were observed, which represents a highly significant microstructural difference. Therefore, considering the presented results, we suggest that there is strong evidence for a correlation between the stress in the lattice and the changes in the capacitance values. The stress originates from the initial state of metal ions in the precursor solution that leads to change in the calcination kinetics and, as a consequence, in grain nucleation and growth.

Conclusions

In conclusion, the results lead us to propose that the order of addition of reagents leads to the existence of different complex metallic ions in the polymeric precursor solution. The obtained oxides have the same morphology, but X-ray diffraction patterns show that the lattice is highly stressed when comparing both of the obtained materials. The observed stress is sufficiently high to explain the capacitance change of both samples.

References

1. Huggins RA (2004) Solid State Ionics 134:179
2. Conway BE (1991) J Electrochem Soc 138:1539
3. Aricó AS, Bruce P, Scrosati B, Arascon JMT, Schalwijk WV (2005) Nat Mater 04:366
4. Pekala RW, Farmer JC, Alviso CT, Tran TD, Mayer ST, Miller JM et al (1998) J Non-Cryst Solids 225:74
5. Honda Y, Haramoto T, Takeshige M, Shiozaki H, Kitamura T, Ishikawa M (2007) Electrochem Solid-State Lett 10:A106
6. Lukaszewsk M, Zurowsk A (2008) Czerwinski A 158:1598
7. Mi H, Zhang X, Yang S, Ye X, Luo J (2008) Mater Chem Phys 112:127
8. Jurewicz K, Delpeux S, Bertagna V, Béguin F, Frackowiak E (2001) Chem Phys Lett 347:36

9. Fabio AD, Giorgi A, Mastragostino M, Soavi F (2001) J Electrochem Soc 148:A845
10. Grupioni AAF, Arashiro E, Lassali TAF (2002) Electrochim Acta 48:407
11. Yang XH, Wang YG, Xiong HM, Xia YY (2007) Electrochim Acta 53:752
12. Hu CC, Chang KH, Wang CC (2007) Electrochim Acta 52:4411
13. Zheng YZ, Ding HY, Zhang ML (2009) Mat Res Bull 44:403
14. Chang KH, Hu CC, Chou CY (2009) Electrochim Acta 54:978
15. He XJ, Geng YJ, Oke S, Higashi K, Yamamoto M, Takikawa H (2009) Synth Metals 159:7
16. Hu CC, Liu MJ, Chang KH (2008) Electrochim Acta 53:2679
17. Conway BE (1999) Electrochemical supercapacitors: scientific fundamentals and technological applications. Plenum, New York
18. Zheng JP, Jow TR (1995) J Electrochem Soc 142:L6
19. Zheng JP, Cygan PJ, Jow TR (1995) J Electrochem Soc 142:2699
20. Park BO, Lokhande CD, Park HS, Jung KD, Joo OS (2004) J Power Sources 134:148
21. Jiang R, Huang T, Liu J, Zhuang J, Yu A (2009) Electrochim Acta 54:3047
22. Chang KH, Hu CC, Chou CY (2007) Chem Mater 19:2112
23. Wang CC, Hu CC (2005) Electrochim Acta 50:2573
24. Liang YY, Liang HL, Zhang XG (2007) J Power Sources 173:599
25. Patake VD, Lokhande CD (2008) Appl Surf Sci 254:2620
26. Pechini MP (1967) Patent EUA No. 3.330.697
27. Santos MC, Terezo AJ, Fernandes VC, Pereira EC, Bulhões LOS (2005) J Solid State Electrochem 9:91
28. Terezo AJ, Pereira EC (2002) Mat Lett 53:339–345
29. Rosario AV, Pereira EC (2005) J Solid State Electrochem 9:665
30. Pocrifka LA, Gonçalves C, Grossi P, Colpa PC, Pereira EC (2006) Sem Act B 113:1012
31. Silva GM, Lemos SG, Pocrifka LA, Marreto PD, Rosário AV, Pereira EC (2008) Anal Chim Acta 616:36
32. Rosário AV, Bulhões LOS, Pereira EC (2006) J Power Sources 158:795
33. Larson AC, Von Dreele RB (2000) General structure analysis system (GSAS). Los Alamos Nat Lab Report LAUR 86–748
34. Toby BH (2001) J Appl Crystallogr 34:210
35. Trasati S, Lodi G (1980) In: Trasatti S (ed) Electrodes of conductive metallic oxide, part A. New York, Elsevier
36. Ardizzone S, Fregonara S, Trasatti S (1990) Electrochim Acta 35:263
37. Hu CC, Chang KH (2002) J Power Sources 112:401
38. Hu CC, Huang YH, Chang KH (2002) J Power Sources 108:117
39. Miller JM, Dunn B, Tran TD, Pekala RW (1997) J Electrochem Soc 144:L309
40. Long JW, Swider KE, Merrzbacher CI, Rolison DR (1999) Langmuir 15:780
41. Kakihana M (1996) J Sol-Gel Sci Technol 6:7
42. Rosario AV, Pereira EC (2006) J Sol-Gel Sci Technol 38:233
43. Nogueira AF, Toma SH, Vidotti M, Formiga ALB, Torresi SIC, Toma HE (2005) New J Chem 29:320
44. Toma SH, Uemi M, Nikolaou S, Tomazela DM, Eberlin MN, Toma HE (2004) Inorg Chem 43:3521